water

MDPI

Article

The Impact of Sediment–Water Ratio and Hydraulic Residence Time on the Release of Inorganic Nitrogen from Sediments in the Pearl River Delta

Zerui Gong [1], Yanling Wang [1], Heping Hu [2], Pengfei Chen [1], Yao Lu [1], Lei Wang [1] and Shaobin Huang [1,*]

[1] School of Environment and Energy, South China University of Technology, Guangzhou 510006, China
[2] China Water Resources Pearl River Planning Surveying & Designing Co., Ltd., Guangzhou 510610, China
* Correspondence: chshuang@scut.edu.cn; Tel.: +86-13527787077

Abstract: Black-odorous water bodies in the Pearl River Delta have been treated. However, the re-release of nitrogen (N)-containing compounds in sediment can cause a relapse of black-odorous water bodies. Sediment–water ratio (SWR) and hydraulic residence time (HRT) influence pollutant release. Therefore, how to control SWR and HRT during the treatment process has become an urgent problem. This study focuses on the dynamic release of endogenous inorganic N from sediments into overlying water in a river channel of Dongguan City, Guangdong Province. Physicochemical parameters (dissolved inorganic nitrogen (DIN), NH_4^+-N, NO_3^--N, NO_2^--N, dissolved oxygen (DO), pH, oxidation-reduction potential (ORP), chemical oxygen demand (COD), Fe and total phosphorus (TP)) of overlying water were monitored under different SWRs (0.71, 0.38, and 0.16) and HRTs (13 days and 6.5 days), and the nitrogen release flux under different conditions was compared. Finally, the correlation and influence pathways among environmental factors were analyzed. The results showed that SWR significantly affected DO, pH, ORP, and sediment N release fluxes while prolonging HRT-promoted denitrification. DIN → NO_2^--N → DO pathway had a total effect of 19.6%, and DIN may promote low DO concentration via NO_2^- oxidation. Maintaining reasonable SWR and HRT can reduce the release of inorganic N from sediment into the overlying water. This study provides a theoretical basis for controlling black-odorous water bodies.

Keywords: black-odorous water bodies; sediment–water ratio; hydraulic residence time; inorganic nitrogen; Pearl River Delta

Citation: Gong, Z.; Wang, Y.; Hu, H.; Chen, P.; Lu, Y.; Wang, L.; Huang, S. The Impact of Sediment–Water Ratio and Hydraulic Residence Time on the Release of Inorganic Nitrogen from Sediments in the Pearl River Delta. *Water* **2023**, *15*, 1789. https://doi.org/10.3390/w15091789

Academic Editor: Alistair Borthwick

Received: 1 April 2023
Revised: 1 May 2023
Accepted: 3 May 2023
Published: 7 May 2023

1. Introduction

The Pearl River Delta is one of China's most developed regions. In recent years, rapid development in the Pearl River Delta has caused a significant increase in pollution from excessive nitrogen (N) discharge due to fertilizer and fossil fuel use [1]. The discharge of wastewater from various sources—such as industrial emissions, agricultural production, urbanization, and human activities—combined with high water temperatures ranging from 13.9 °C in winter to 31.5 °C in summer has resulted in black-odorous water bodies, unique to southern China [2,3]. The Pearl River Delta region—part of Guangdong Province—records the highest number of black-odorous water bodies in China. According to data collected from the National Urban Black-odorous Waterbodies Governance and Supervision Platform (Chinese Ministry of Housing and Urban-rural Development, 2020), there were almost 250 black-odorous water bodies in Guangdong Province, with 41 still untreated. Algae and bacteria activity in Guangzhou and Hong Kong have also transformed some riverbed sediment into black-odorous sediment [4,5]. Therefore, measures have been put in place to treat black-odorous water bodies. However, pollutants can still desorb from sediment and diffuse into the overlying water under certain conditions, leading to the recurrence of black-odorous water bodies under certain conditions [6,7]. For example, disturbance or changes in oxidation-reduction potential (ORP) and pH values of sediment can cause

pollutants to migrate into the overlying water, leading to a relapse of black-odorous water bodies [8,9]. High levels of dissolved inorganic N can also cause blue-green algae growth and eutrophication [10,11]. In addition, the process of dissimilatory nitrate reduction to ammonium (DNRA) can transform NO_3^- into ammonia (NH_3) [12]. Increased organic matter (OM) deposition and oxygen consumption on the surface of nutrient-rich sediment systems result in a more reduced state, affecting the biogeochemistry and nutrient cycling of sediment [13–16]. As shown by the document "Letter on the notification of the national water environment situation in the first half of 2022" from the General Office of the Ministry of Ecology and Environment, in the first half of 2022, 10 cities in China with completed black-odorous water body remediation reported significant relapse, with two of them located in the Pearl River Delta region. Thus, it is necessary to study environmental factors affecting sediment pollutant release to control water quality.

Sediment–water ratio (SWR)—the ratio of sediment thickness to overlying water depth—is a critical factor affecting pollutant distribution in sediments and overlying water. Previous studies have shown that changes in SWR induced by rainfall and human activities—such as dredging, rainfall, and wastewater discharge events—can significantly alter pollutant loadings in aquatic systems [17–19]. Typically, pore water in sediment serves as a carrier of sediment pollutants, while overlying water is the endpoint for pollutant migration. Thus, sediment thickness directly affects the total amount of pollutants, while overlying water volume affects pollutant concentration [20]. To date, most research in SWR has been focused on coastal and marine systems [21,22] with little attention paid to freshwater ecosystems in South China. Hydraulic residence time (HRT)—on the other hand—is an important parameter in water environmental engineering, representing the average time that overlying water stays in the system [23]. HRT is mainly determined by the flow rate and the cross-sectional area of the river. A reduction in HRT can trigger hydrodynamic shear force, turbulence, and sediment resuspension at the sediment–water interface (SWI) [24,25], which can alter nutrient and oxygen transport processes, thus affecting the microbial habitats crucial for the survival of aquatic organisms and plants [26,27]. The initial occurrence of low dissolved oxygen (DO) in the water column takes place at the SWI [28], where iron oxides dissolve and release iron into the pore water under reducing conditions [29,30]. Therefore, the process of blackening originates from the SWI and spreads towards the water body [31]. Previous studies have reported that controlling SWR and reducing HRT can effectively reduce pollution from the SWI in estuaries, lakes, coastal regions, and marine systems [32–35]. Nevertheless, the impact of different SWRs and HRTs on water quality and pollutant distribution in freshwater ecosystems in South China still needs to be further investigated, and a statistical analysis of the effects of SWR and HRT on water quality is currently lacking.

To investigate the dynamic sediment release rules under different SWRs and HRTs, we conducted a 53-day experiment where black-odorous sediment from the Pearl River Delta was added to three dynamic overlying water sediment (DOWS) systems, simulating and analyzing N (dissolved inorganic nitrogen (DIN), NH_4^+-N, NO_3^--N and NO_2^--N) release flux and patterns of sediment into overlying water under different SWRs and HRTs. We monitored changes in physicochemical parameters—including DO, pH, ORP, chemical oxygen demand (COD), Fe, and total phosphorus (TP)—and analyzed their correlations with preset and water quality parameters. This study aims to provide theoretical support for controlling the relapse of black-odorous water bodies.

2. Materials and Methods

2.1. Sediments

As shown in Figure 1, the experiment selected sediment from the Xiacao River (23°1′17″, 113°37′51″), located in Wangniudun Town, Dongguan City, Guangdong Province, China. This river has formed black-odorous water bodies due to excessive discharge of metal and electronic wastewater, with a large amount of iron oxide visible on the water surface and a strong odor. A box corer was used during sediment collection, and sediment

was collected up to a depth of 50 cm from the surface and immediately transported back to the laboratory within 4 h. To ensure comparability, debris such as garbage and branches in the sediment were removed before starting the experiment.

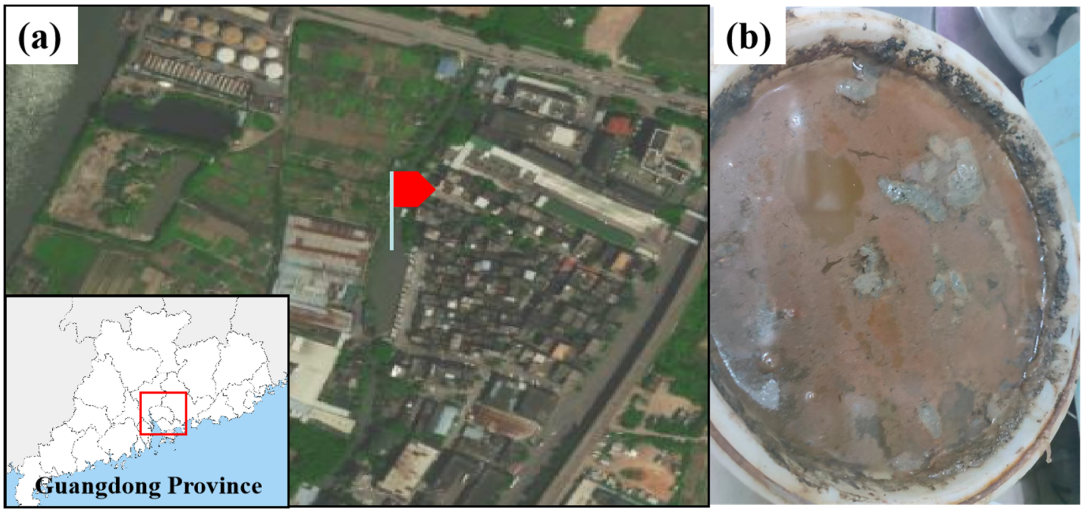

Figure 1. (**a**) Sampling location. The location marked by the flag is the sampling point. (**b**) Sediment collected.

2.2. Set-Up

As shown in Figure 2, three DOWS systems were constructed in the laboratory using three organic glass columns (1.5 m high and 0.14 m inner diameter), a water tank, and a peristaltic pump (BT100-2J, Longer Precision Pump Co., Ltd., Baoding, China). Homogenized sediment was added to the bottom of each DOWS with controlled sediment thicknesses of 60 cm, 40 cm, and 20 cm, respectively, named DOWS1, DOWS2, and DOWS3. Deionized water was added before the start of the experiment, the water inlet of each DOWS was placed 3 cm above the SWI, and an overflow outlet was set at a height of 145 cm in each DOWS to maintain the depth of the overlying water at 85 cm, 105 cm, and 125 cm, respectively, resulting in SWRs of 0.71, 0.38 and 0.16. The peristaltic pump operated at a constant rate to ensure a continuous flow of the overlying water and compensate for water loss due to evaporation and sampling.

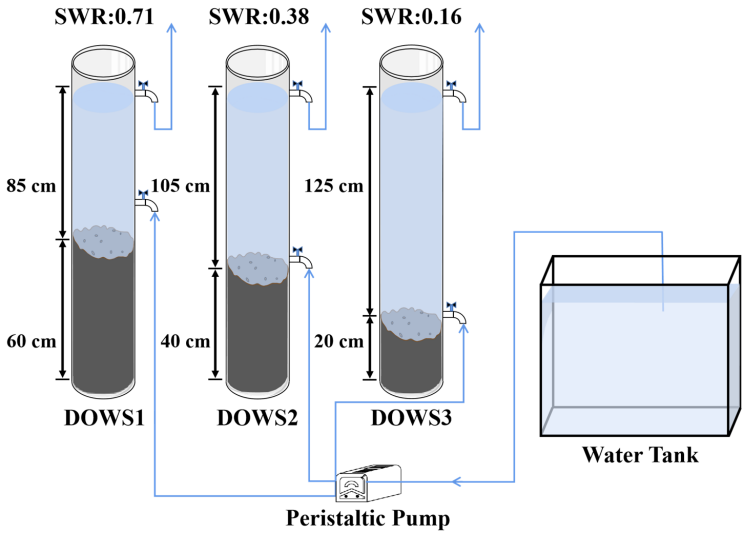

Figure 2. Diagram of the experimental set-up.

2.3. Operation

According to the different HRT of the overlying water, the experimental period was divided into two stages, named stage 1 (days 1–35) and stage 2 (days 37–53). In stage 1, the HRT was 13 days, and the flow rates of DOWS1, DWOS2, and DOWS3 were 0.70, 0.86, and 1.03 mL·min^{-1}, respectively; in stage 2, the HRT was 6.5 days, and the flow rates of DOWS1, DWOS2, and DOWS3 were 1.40, 1.72, and 2.06 mL·min^{-1}, respectively. The flow rate of the overlying water was controlled by a precision peristaltic pump.

The relationship between HRT and overlying water flow rate is expressed as:

$$\mathrm{HRT} = \frac{10^5 \times H \times \pi d^2}{576 \times Q} \quad (1)$$

where H represents the depth of the overlying water (m), d represents the inner diameter of the dynamic overlying water sediment (DOWS) (m) and Q represents the inlet flow rate of the DOWS (mL·min^{-1}).

2.4. Physicochemical Indexes

In our experiment, the Chinese National Standard methods were used to detect the concentrations of NH_4^+-N, NO_3^--N, NO_2^--N, COD, TP, and Fe in the water samples. The methods are described as follows: NH_4^+-N in water samples was detected according to the method specified in GB 7481-87, using Nessler's reagent colorimetry. NO_3^--N was determined according to the procedures outlined in GB 11894-89 using reduction by cadmium and colorimetric detection with salicylic acid. NO_2^--N was detected by the method prescribed in GB 748-87, using sulfanilic acid and N-(1-Naphthyl)ethylenediamine dihydrochloride diazo chromogenic reaction. COD was analyzed with the potassium dichromate method outlined in GB 11914-89. TP was detected according to the procedures specified in GB 11893-89, using H_2SO_4 digestion and ammonium molybdate spectrophotometric analysis. The concentration of Fe was detected according to the procedures specified in GB 11892-89, using the 1,10-phenanthroline method.

Water samples below 20 cm from the water surface were collected periodically and filtered through a 0.45 µm filter. The concentrations of NH_4^+-N, NO_3^--N, NO_2^--N, COD, and TP were analyzed using a UV-visible spectrophotometer (EPOCH2 microplate reader, BioTek Instruments, Santa Clara, CA, USA). DIN was determined as the sum of NH_4^+-N, NO_3^--N, and NO_2^--N. ORP was measured using an ORP electrode (501-ORP, Leici Instrument Branch of Shanghai Yidian Scientific Instrument Co., Ltd., Shanghai, China). DO measurements were conducted in situ using a portable multi-parameter analyzer (JPSJ-605F, Leici Instrument Branch of Shanghai Yidian Scientific Instrument Co., Ltd., Shanghai, China), while pH was determined using a pH meter (PHS-3E, INESA Scientific Instrument Co., Ltd., Shanghai, China). Each sample was measured three times.

2.5. Data Statistics and Analysis

Statistical analysis was performed using IBM SPSS Statistics 22 (IBM, New York, NY, USA) and R version 4.2.1 (www.r-project.org accessed on 23 June 2022), and charts were generated using Origin 2023. The non-parametric Friedman test was used to determine the mean and statistical differences among the experimental results of each DOWS to check for differences between SWRs. When a statistically significant p-value (<0.05) was obtained from the Friedman test, Wilcoxon signed-rank test was conducted, whose advantage is that it does not require distributional assumptions, can handle small sample sizes and outliers, and is useful when the data are not normally distributed [36,37]. To assess whether the changes in HRT significantly impacted the physicochemical parameters, we conducted Wilcoxon signed-rank tests on each DOWS across various HRT conditions. Spearman rank correlation analysis was performed using R to investigate the correlation between the experimental results of each DOWS. To further explore the relative importance of DO, a best-fit model was established using a multiple-stepwise regression approach to test the overall goodness-of-fit of the model. Path analysis is a structural equation modeling

method used to measure the comprehensive influence of multiple factors on multiple variables. Its advantage is that it allows for direct and indirect effects between variables, considers multiple factors' influence, assesses the overall fit of a model, and can provide a high level of transparency in structural comparisons [38]. During multiple-stepwise regression analysis and path analysis, multicollinearity among environmental variables was diagnosed, and no multicollinearity was found (variance inflation factor, VIF < 5) [39].

Nutrient fluxes were calculated using Equation (2). Positive values indicate nutrient release from sediment to overlying water, while negative values indicate nutrient sorption by sediment.

$$F = \frac{1000 \times (c_m - c_n) \times V}{\pi\left(\frac{d}{2}\right)^2 \times (m - n)} \quad (2)$$

In Equation (2), F represents nutrient flux ($(mg \cdot (m^2 \cdot d)^{-1})$; m and n represent specific days on which sample collection was conducted during the experiment (d); c_m and c_n represent nutrient concentrations of samples on day m and day n, respectively ($mg \cdot L^{-1}$); V represents the volume of the overlying water (m^3); and d represents the inner diameter of DOWS (m).

3. Results and Discussion

3.1. Significance of Physicochemical Parameter Differences under Different SWR and HRT

The Friedman test results for various physicochemical parameters among different SWRs and the Wilcoxon signed-rank test results for various physicochemical parameters among different HRTs are shown in Table 1. As shown in the table, during stage 1, significant concentration differences were observed for DO, pH, and NO_2^--N among different SWRs ($p < 0.05$). During stage 2, significant differences above the level of significance were observed for DO, pH, and ORP among different SWRs ($p < 0.01$). The differences in DO and pH were most significant across different SWRs, which can be attributed to variations in microbial abundance within sediments under different SWRs. DO and pH can affect the ability of microorganisms to adapt and metabolize within sediments, therefore influencing oxygen consumption rates and organic matter degradation in sediment–water systems [40,41]. Physicochemical parameters, shown in Figures 3 and 4, typically had lower average values in the second stage than in the first stage. Notably, exceptions to this trend were observed for COD and NH_4^+-N in DOWS1, as well as Fe in DOWS3. Significant differences were observed in DO in DOWS1, COD, NO_3^--N, and TP in DOWS3, as well as ORP values across all DOWS, under different HRT conditions. The response of ORP to changes in HRT was most significant, as longer HRT favors bio-oxidation [42].

Table 1. Test of differences in environmental variables among overlying water depths at the four DOWS of the experiment. Results based on the Friedman test and Wilcoxon Signed Ranks test.

		SWR [a]			**HRT** [b]		
		Stage 1	**Stage 2**		**DOWS1**	**DOWS2**	**DOWS3**
DO	Asymp. Sig.	**0.001** **	**<0.001** ***	Z	−2.578 [c]	−1.023 [c]	−1.156 [c]
	χ^2	13.300	16.545	Asymp. Sig.	**0.010** **	0.306	0.248
pH	Asymp. Sig.	**0.019** *	**0.004** **	Z	−1.423 [c]	−0.356 [d]	−1.245 [c]
	χ^2	7.895	10.857	Asymp. Sig.	0.155	0.722	0.213
ORP	Asymp. Sig.	0.086	**0.004** **	Z	−2.934 [c]	−2.490 [c]	−2.936 [c]
	χ^2	4.900	11.091	Asymp. Sig.	**0.003** **	**0.013** *	**0.003** **
COD	Asymp. Sig.	0.329	0.406	Z	−0.889 [d]	−0.652 [c]	−2.380 [c]
	χ^2	2.225	1.805	Asymp. Sig.	0.374	0.515	**0.017** *
DIN	Asymp. Sig.	0.058	0.695	Z	−1.689 [c]	−1.867 [c]	−1.956 [c]
	χ^2	5.700	0.727	Asymp. Sig.	0.091	0.062	0.050
NH_4^+-N	Asymp. Sig.	0.411	0.070	Z	−1.334 [d]	−1.156 [c]	−1.580 [c]
	χ^2	1.788	5.317	Asymp. Sig.	0.182	0.248	0.114
NO_3^--N	Asymp. Sig.	0.058	0.307	Z	−1.867 [c]	−1.689 [c]	−2.045 [c]
	χ^2	5.700	2.364	Asymp. Sig.	0.062	0.091	**0.041** *

Table 1. *Cont.*

		SWR [a]			HRT [b]		
		Stage 1	**Stage 2**		**DOWS1**	**DOWS2**	**DOWS3**
NO_2^--N	Asymp. Sig.	**0.045** *	0.074	Z	−1.868 [c]	−1.201 [c]	−1.601 [c]
	χ^2	6.200	5.200	Asymp. Sig.	0.062	0.230	0.109
Fe	Asymp. Sig.	0.782	0.148	Z	−0.089 [c]	−0.178 [c]	−0.533 [d]
	χ^2	0.492	3.818	Asymp. Sig.	0.929	0.859	0.594
TP	Asymp. Sig.	0.235	0.241	Z	−0.178 [c]	−1.125 [c]	−1.960 [c]
	χ^2	2.896	2.850	Asymp. Sig.	0.859	0.260	**0.50** *

Notes: Asymp. Sig., asymptotic significance; Z, Z-score; χ^2, Chi-Square; DO, dissolved oxygen (mg·L^{-1}); ORP, oxidation-reduction potential (mV); COD, chemical oxygen demand (mg·L^{-1}); DIN, dissolved inorganic nitrogen (mg·L^{-1}); NH_4^+-N, ammonia nitrogen (mg·L^{-1}); NO_3^--N, nitrate nitrogen (mg·L^{-1}); NO_2^--N, nitrite nitrogen (mg·L^{-1}); Fe (mg·L^{-1}); TP, total phosphorus (mg·L^{-1}). Significant correlations in bold; * indicates a statistical difference, $p < 0.05$; ** indicates a statistically significant difference, $p < 0.01$; *** indicates a highly statistically significant difference, $p < 0.001$. Positive or negative ranks in the table indicate higher or lower values detected in the low-HRT than in the high-HRT. [a] Friedman test. [b] Wilcoxon Signed Ranks test. [c] Based on positive ranks. [d] Based on negative ranks.

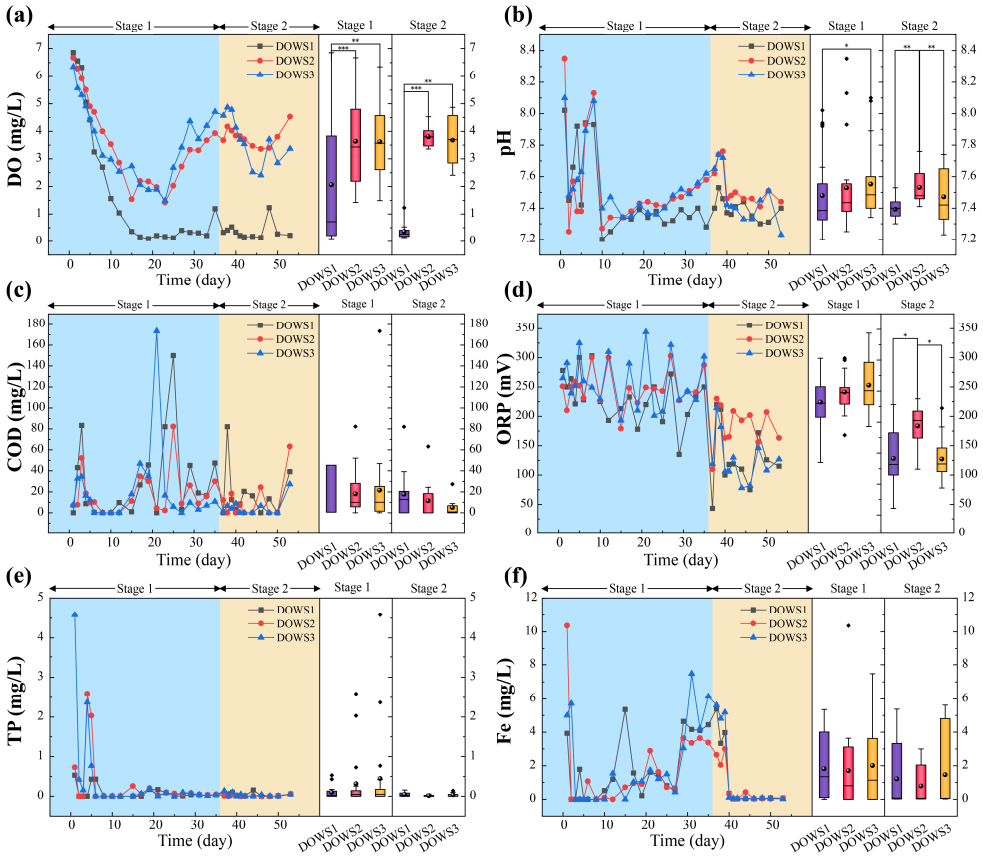

Figure 3. Variation curves and box plots of physicochemical parameters at each sediment–water ratio. Wilcoxon signed-rank tests were performed when the Friedman test gave a highly significant level. (**a**) DO; (**b**) pH; (**c**) COD; (**d**) ORP; (**e**) TP; (**f**) Fe. * indicates a statistical difference, $p < 0.05$; ** indicates a statistically significant difference, $p < 0.01$; *** indicates a highly statistically significant difference, $p < 0.001$.

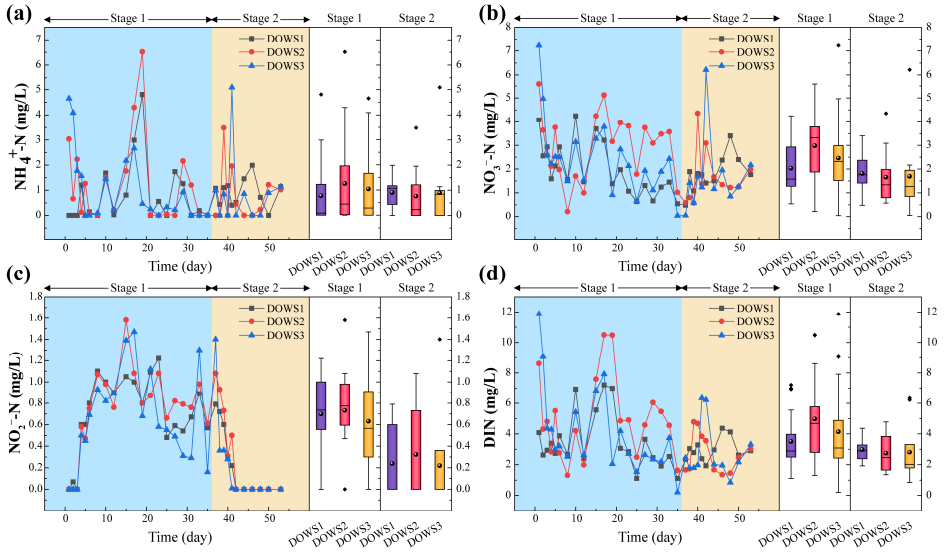

Figure 4. Variation curves and box plots of inorganic nitrogen concentrations at each sediment–water ratio. (**a**) NH_4^+-N; (**b**) NO_3^--N; (**c**) NO_2^--N; (**d**) DIN.

3.2. Changes and Wilcoxon Signed-Rank Test of DO, pH, COD, ORP, Fe, and TP

The changes in DO, pH, COD, ORP, Fe, and TP in the overlying water of each DOWS, as well as the differences between stage 1 and stage 2, are shown in Figure 3.

DO showed a significant concentration gradient and reaeration process under different SWRs, with significantly lower values in DOWS1 than that in DWOS2 and 3 (Figure 3a). After the start of the experiment, the DO concentrations in all DOWS rapidly decreased, with all DOWS maintaining around 6.5 mg·L^{-1} on the first day. However, from the 2nd to the 23rd day, DO rapidly decreased to around 0.1 mg·L^{-1} in DOWS1, while it dropped to around 1.5 mg·L^{-1} in DOWS2 and 3. After the 23rd day, DO did not change significantly in DOWS1, whereas it increased rapidly to around 4.5 mg·L^{-1} in DOWS2 and 3, exhibiting a phenomenon of initial decrease followed by an increase after HRT was shortened. These data indicate that the reaeration capacity of the overlying water is inhibited when the SWR is 0.71, and the DO concentration in the overlying water increases as the SWR decreases [43]. The pH value of the overlying water was higher at an HRT of 13 days than at an HRT of 6.5 days, indicating that the longer HRT promotes the production of alkaline substances, which dissolve into the overlying water. In addition, although COD does not exhibit an obvious pattern of change, a decrease was observed after the HRT was shortened. These may be due to a higher proportion of organic matter degradation as Stage 2 DO was lower than Stage 1 DO [44]. Moreover, the concentration of COD in DOWS1 was statistically significantly higher than that in DOWS2 and 3, which may be due to its highest SWR. Moreover, ORP and Fe decreased overall as the HRT was shortened. However, ORP remained at a strong oxidative level throughout the experiment (Figure 3d,e). According to some previous studies, the release of phosphorus (P) from sediments is mainly derived from surface sediments [45], and the amount of P released under alkaline conditions is greater than that released under acidic conditions [41]. These may explain the reason the concentration of TP was initially high but decreased after day 8.

3.3. Changes in DIN, NH_4^+-N, NO_3^--N and NO_2^--N

Sediment is a crucial N storage reservoir that can release nutrients to overlying water under certain conditions. Inorganic N serves as an essential nutrient for aquatic organisms; thus, investigating the N flux at the SWI has significant ecological implications. The changes in DIN, NH_4^+-N, NO_3^--N, and NO_2^--N concentrations in each DOWS and the differences between stage 1 and stage 2 are presented in Figure 4.

The results indicated that there were no statistically significant differences in the concentration of each parameter among different DOWS or stages ($p > 0.05$). During stage

1, the concentrations of DIN, NH_4^+-N, and NO_3^--N were slightly higher in DOWS2 than in DOWS1 and 3. Although the Friedman test for NO_2^--N during stage 1 was significant, the *p*-values between DOWS for NO_2^--N were all greater than 0.05 after the Wilcoxon signed-rank test was performed.

The characteristics of the changes at different stages showed that the average concentrations of DIN, NH_4^+-N, NO_3^--N, and NO_2^--N were highest during stage 1 and lowest during stage 2. The average values of DIN, NH_4^+-N, NO_3^--N, and NO_2^--N in DOWS2 during stage 1 were 1.81, 1.65, 1.80, and 2.27 times those during stage 2, respectively. The increase in NO_2^--N during stage 1 was accompanied by a decrease in DO and ORP, while during stage 2, NO_2^--N continued to decrease despite lower DO, indicating the occurrence of anaerobic denitrification [46]. The sustained decrease in NO_2^--N during stage 2 may also be due to the shortened HRT and decreased COD, resulting in insufficient denitrification strength [47]. During stage 1, the peak and average values of DIN, NH_4^+-N, and NO_3^--N in DOWS2 were higher than those in DOWS1 and 3. In the entire experiment, the concentrations of DIN and NO_3^--N in the overlying water under two different HRTs have decreased, which may be attributed to the presence of denitrification. In addition, previous studies have indicated that increased organic carbon and nitrogen content can promote ammonium release [48,49]. These suggested that sediment—with its rich functional microorganisms—may play a dual role as a source of pollutants and a site for microbial removal. Therefore, SWR and HRT can lead to differences in N concentrations in the overlying water.

In addition, the fluctuation in N release flux during stage 1 was more significant than during stage 2 (Figure 5). However, there was no significant difference in the mean and median N release flux between the two HRTs. The variation of DIN flux is more sensitive to HRT changes relative to NH_4^+-N and NO_3^--N. N flux in this study holds great significance for practical applications. However, the simulation experiment yielded nitrogen flux values higher than those observed in reality, possibly due to greater sediment contamination levels in the simulation [50].

3.4. The Relationship between Nutrients and Potential Influencing Factors

To illustrate the relationship between nutrients and potential influencing factors, we performed Spearman rank correlation analysis, and the results are shown in Figure 6. As shown in the figure, during stage 1, DIN was significantly correlated with NH_4^+-N in all DOWS and extremely significantly correlated with NO_3^--N. DO was negatively correlated only with NO_2^--N. The dissolved oxygen (DO) concentration in the overlying water has been demonstrated to affect denitrification in aquatic systems. Molecular oxygen can inhibit the activity of denitrifying enzymes, especially nitrite reductase [51].

DO is an important parameter that affects microbial metabolic function, and it is usually a key parameter in controlling nitrification, denitrification processes, and OM degradation efficiency in wastewater treatment [52]. The stepwise multiple regression results between DO concentration and potential influencing variables are shown in Table 2. During multiple-stepwise regression analysis, no multicollinearity was found among environmental variables (ORP, COD, pH, NH_4^+-N, NO_3^--N, NO_2^--N, Fe, and TP). During stage 2, no variables entered the equation for DOWS1; DO was positively correlated with ORP in DOWS2, explaining 41% of the variance; DO was positively correlated with ORP but negatively correlated with NO_2^--N in DOWS3, explaining 84% of the variance. These models could well fit the DO concentration in DOWS3 during stage 2 and describe the potential influence well. These results further indicate that pH, ORP, DIN, NO_3^--N, and NO_2^--N have a significant impact on DO concentration.

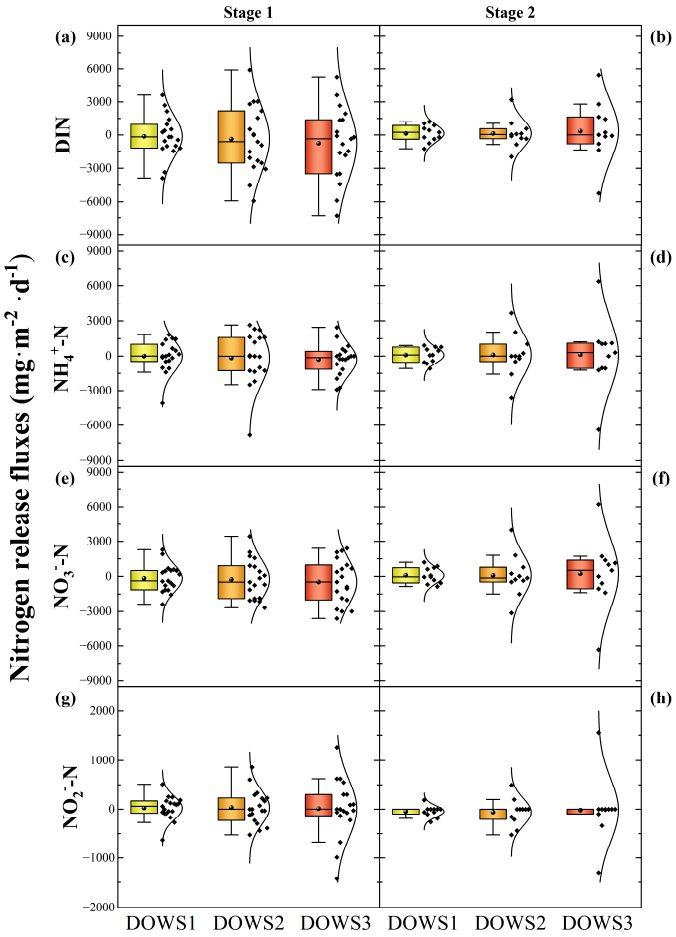

Figure 5. Nitrogen release fluxes at different stages (HRTs) ($mg \cdot m^{-2} \cdot d^{-1}$). (**a**) DIN in Stage 1; (**b**) DIN in Stage 2; (**c**) NH_4^+-N in Stage 1; (**d**) NH_4^+-N in Stage 2; (**e**) NO_3^--N in Stage 1; (**f**) NO_3^--N in Stage 2; (**g**) NO_2^--N in Stage 1 (**h**) NO_3^--N in Stage 2.

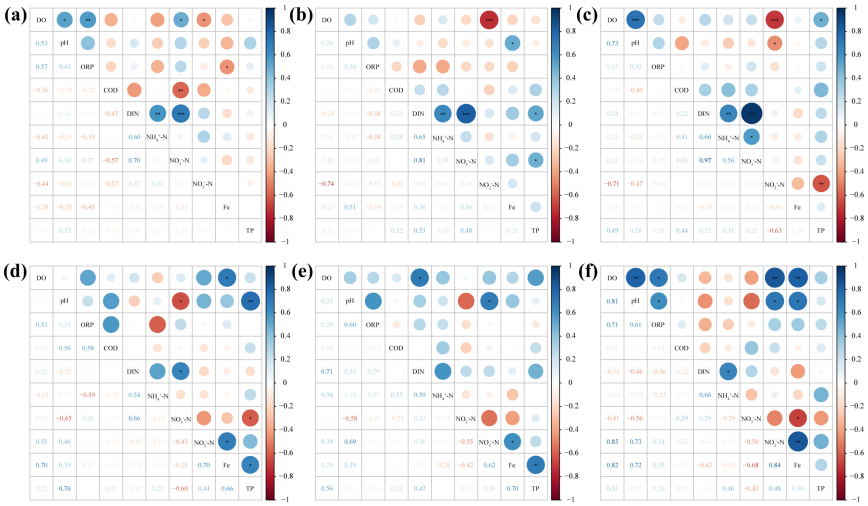

Figure 6. Spearman rank correlations. Spearman's correlation coefficients between environmental variables were expressed in color gradient and circle size. Boxplot was used to observe the overall distribution of data. (**a**–**c**) represent DOWS 1, 2, and 3 in Stage 1, respectively, and (**d**–**f**) represent DOWS 1, 2, and 3 in Stage 2, respectively. * indicates a statistical difference, $p < 0.05$; ** indicates a statistically significant difference, $p < 0.01$; *** indicates a highly statistically significant difference, $p < 0.001$.

Table 2. Multiple-stepwise regression of DO with the potential influencing variables (PIN(0.050), POUT(0.100)).

		Step	R^2	F	p	Equation
Stage 1	DOWS1	1	0.491	19.335	<0.001	DO = −4.855 (±1.104) NO_2^--N + 5.457 (±0.864)
		2	0.712	24.464	<0.001	DO = −3.818 (±0.874) NO_2^--N + 4.678 (±1.217) pH + 30.263 (±9.312)
		3	0.773	22.606	<0.001	DO = −3.765 (±0.775) NO_2^--N + 4.046 (±1.112) pH + 0.572 (±0.241) NO_3^--N − 26.734 (±8.392)
	DOWS2	1	0.646	35.735	<0.001	DO = −3.298 (±0.552) NO_2^--N + 6.048 (±0.456)
	DOWS3	1	0.434	15.561	<0.001	DO = −1.724 (±0.489) NO_2^--N + 2.266 (±0.990) pH − 12.404 (±7.572)
		2	0.544	12.352	<0.001	DO = −1.524 (±0.451) NO_2^--N + 2.111 (±0.897) pH + 0.308 (±0.140) NH_4^+-N − 11.688 (±6.850)
Stage 2	DOWS1	No variables entered				
	DWOS2	1	0.408	7.885	0.020	DO = 12.817 (±4.564) TP + 3.628 (±0.101)
	DOWS3	1	0.620	14.705	0.004	DO = 0.017 (±0.004) ORP + 1.572 (±0.575)
		2	0.836	20.360	<0.001	DO = 0.015 (±0.003) ORP − 0.967 (±0.299) NO_2^--N + 1.607 (±0.401)

The benthic release of DIN may stimulate primary production and oxygen consumption in aquatic systems [53]. Therefore, a pathway analysis was conducted to investigate the influence of DIN on DO. The results of the path analysis are shown in Figure 7. According to the results of χ^2, p, and CFI values, the path model for DOWS1 during stage 1 was acceptable. Overall, when pH, NO_3^--N, and NO_2^--N were included in the model, 42.6% of DIN variation was considered. When ORP and NO_2^--N were included in the model, 23.0% of DIN variation was considered. The path coefficients from DIN to NO_3^--N and from NO_3^--N to DO were positive, indicating that DIN indirectly promoted DO by increasing NO_3^--N (total effect = 20.6%). Based on the positive correlation between DIN and NO_2^--N combined with the negative correlation between NO_2^--N and DO, it can be inferred that DIN may promote the consumption of a large amount of DO by promoting NO_2^- oxidation, therefore maintaining low DO concentration (total effect = 19.6%) [54].

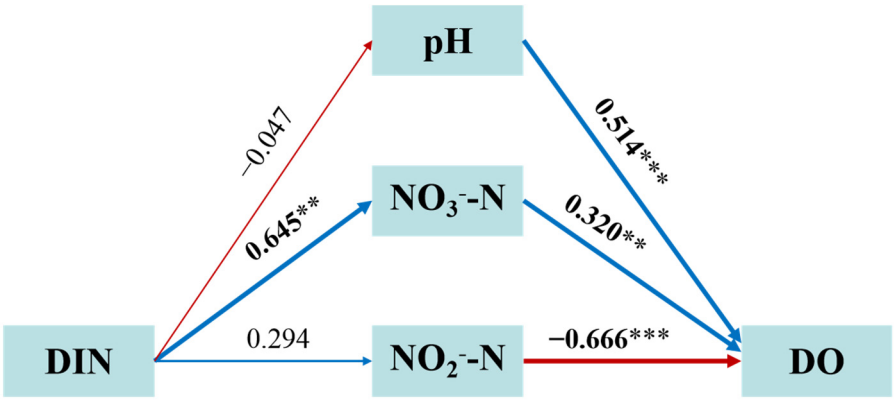

Figure 7. The path analysis diagram depicts the DIN to DO influence process for DOWS1 of Stage 1. The single-headed arrows represent unidirectional cause-effect relationships. The thickness of the line indicates the strength of the correlation, and the numbers adjacent to the arrows are standardized path coefficients (significant correlations in bold). The red and blue lines represent significant negative and positive paths, respectively. ** indicates a statistically significant difference, $p < 0.01$; *** indicates a highly statistically significant difference, $p < 0.001$.

4. Conclusions

The main conclusions can be summarized as follows:

- In DOWS, sediment is a potential source and transformation site of pollutants. Sediment can not only adsorb and precipitate pollutants but also release and transform them.

- SWR is positively correlated with DO in the overlying water and negatively correlated with COD, directly affecting the N release flux from the sediment. N-containing compounds in sediment can be transformed into various forms of N through microbial reactions and released into the overlying water.
- Shortening HRT may lead to weakened denitrification capacity in DOWS.
- DIN promotes NO_2^- oxidation—which consumes DO in the overlying water—maintaining DO concentration at a lower level.
- Thus, the SWR and HRT jointly determine the outcome of the overlying water quality. In the future, greater attention should be paid to the roles of SWR and HRT in nutrient-release processes from sediments. This study can provide a theoretical basis for controlling the reversion of black-odorous water bodies.

Author Contributions: Conceptualization, Z.G., Y.W., H.H. and S.H.; methodology, Z.G. and Y.W.; software, P.C.; investigation, Z.G., Y.W. and L.W.; resources, H.H.; data curation, Y.W.; writing—original draft preparation, Z.G. and Y.W.; writing—review and editing, P.C. and Y.L.; visualization, P.C.; supervision, S.H.; project administration, S.H.; funding acquisition, S.H. All authors have read and agreed to the published version of the manuscript.

Funding: This research was funded by the Research Project of the National Natural Science Foundation of China (Grant number 52270105) and the Science and Technology Innovation Program from Water Resources of Guangdong Province (Grant number No. 2023-03).

Data Availability Statement: The data presented in this study are available on request from the corresponding author.

Conflicts of Interest: The authors declare no conflict of interest.

References

1. Galloway, J.N.; Dentener, F.J.; Capone, D.G.; Boyer, E.W.; Howarth, R.W.; Seitzinger, S.P.; Asner, G.P.; Cleveland, C.C.; Green, P.A.; Holland, E.A.; et al. Nitrogen Cycles: Past, Present, and Future. *Biogeochemistry* **2004**, *70*, 153–226. [CrossRef]
2. He, Q.; Xie, Z.; Tang, M.; Fu, Z.; Ma, J.; Wang, H.; Zhang, W.; Zhang, H.; Wang, M.; Hu, J.; et al. Insights into the simultaneous nitrification, denitrification and phosphorus removal process for in situ sludge reduction and potential phosphorus recovery. *Sci. Total Environ.* **2021**, *801*, 149569. [CrossRef] [PubMed]
3. Zhu, D.; Cheng, X.; Sample, D.J.; Yazdi, M.N. The effect of temperature on sulfate release from Pearl River sediments in South China. *Sci. Total Environ.* **2019**, *688*, 1112–1123. [CrossRef]
4. Goodkin, N.; Switzer, A.D.; Mccorry, D.; DeVantier, L.; True, J.D.; Hughen, K.A.; Angeline, N.; Yang, T.T. Coral communities of Hong Kong: Long-lived corals in a marginal reef environment. *Mar. Ecol. Prog. Ser.* **2011**, *426*, 185–196. [CrossRef]
5. Fu, F.; Huang, S.; Hu, H.; Yao, L.; Wang, Y.; Yuan, J.; Gong, Z.; Wu, J.; Zhang, Y. Transformation of N and S pollutants and characterization of microbial communities in constructed wetlands with *Vallisneria natans*. *J. Water Process Eng.* **2021**, *42*, 102186. [CrossRef]
6. Li, Z.; Sheng, Y.; Yang, J.; Burton, E.D. Phosphorus release from coastal sediments: Impacts of the oxidation-reduction potential and sulfide. *Mar. Pollut. Bull.* **2016**, *113*, 176–181. [CrossRef] [PubMed]
7. Peng, C.; Huang, Y.; Yan, X.; Jiang, L.; Wu, X.; Zhang, W.; Wang, X. Effect of overlying water pH, temperature, and hydraulic disturbance on heavy metal and nutrient release from drinking water reservoir sediments. *Water Environ. Res.* **2021**, *93*, 2135–2148. [CrossRef]
8. Bareket, M.M.; Bookman, R.; Katsman, R.; Stigter, H.; Herut, B. The role of transport processes of particulate mercury in modifying marine anthropogenic secondary sources, the case of Haifa bay, Israel. *Mar. Pollut. Bull.* **2016**, *105*, 286–291. [CrossRef]
9. Hu, T.; Shi, M.; Mao, Y.; Liu, W.; Li, M.; Yu, Y.; Yu, H.; Cheng, C.; Zhang, Z.; Zhang, J.; et al. The characteristics of polycyclic aromatic hydrocarbons and heavy metals in water and sediment of dajiuhu subalpine wetland, shennongjia, central China, 2018-2020: Insights for sources, sediment-water exchange, and ecological risk. *Chemosphere* **2022**, *309*, 136788. [CrossRef]
10. Herbeck, L.S.; Unger, D.; Wu, Y.; Jennerjahn, T.C. Effluent, nutrient and organic matter export from shrimp and fish ponds causing eutrophication in coastal and back-reef waters of NE Hainan, tropical China. *Cont. Shelf Res.* **2013**, *57*, 92–104. [CrossRef]
11. Howarth, R.W.; Marino, R. Nitrogen as the limiting nutrient for eutrophication in coastal marine ecosystems: Evolving views over three decades. *Limnol. Oceanogr.* **2006**, *51*, 364–376. [CrossRef]
12. Jiang, M.; Feng, L.; Zheng, X.; Chen, Y. Bio-denitrification performance enhanced by graphene-facilitated iron acquisition. *Water Res.* **2020**, *180*, 115916. [CrossRef] [PubMed]
13. Smolders, A.J.P.; Lamers, L.P.M.; Lucassen, E.C.H.E.; Van Der Velde, G.; Roelofs, J.G.M. Internal eutrophication: How it works and what to do about it—A review. *Chem. Ecol.* **2006**, *22*, 93–111. [CrossRef]
14. Conley, D.J.; Humborg, C.; Rahm, L.; Savchuk, O.P.; Wulff, F. Hypoxia in the Baltic Sea and Basin-Scale Changes in Phosphorus Biogeochemistry. *Environ. Sci. Technol.* **2002**, *36*, 5315–5320. [CrossRef] [PubMed]

15. Friedl, G.; Dinkel, C.; Wehrli, B. Benthic fluxes of nutrients in the northwestern Black Sea. *Mar. Chem.* **1998**, *62*, 77–88. [CrossRef]
16. Pratihary, A.K.; Naqvi, S.W.A.; Naik, H.; Thorat, B.R.; Narvenkar, G.; Manjunatha, B.R.; Rao, V.P. Benthic fluxes in a tropical Estuary and their role in the ecosystem. *Estuar. Coast. Shelf Sci.* **2009**, *85*, 387–398. [CrossRef]
17. Soetan, O.; Nie, J.; Feng, H. Preliminary environmental assessment of metal-contaminated sediment dredging in an Urban River, New Jersey, USA. *Mar. Pollut. Bull.* **2022**, *184*, 114212. [CrossRef] [PubMed]
18. Pires, A.P.F.; Marino, N.A.C.; Srivastava, D.S.; Farjalla, V.F. Predicted rainfall changes disrupt trophic interactions in a tropical aquatic ecosystem. *Ecology* **2016**, *97*, 2750–2759. [CrossRef] [PubMed]
19. Wang, X.; Li, J.; Li, Y.; Shen, Z.; Wang, X.; Yang, Z.; Lou, I. Is urban development an urban river killer? A case study of Yongding Diversion Channel in Beijing, China. *J. Environ. Sci.* **2014**, *26*, 1232–1237. [CrossRef] [PubMed]
20. Wen, M.; Shan, H.; Zhang, S.; Liu, X.; Jia, Y. Contribution of waves and currents to sediment resuspension in the Yellow River Delta. *Mar. Georesour. Geotechnol.* **2019**, *37*, 96–102. [CrossRef]
21. Yousif, R.; Warren, C.; Ben-Hamadou, R.; Husrevoglu, S. Modeling sediment transport in Qatar: Application for coastal development planning. *Integr. Environ. Assess. Manag.* **2018**, *14*, 240–251. [CrossRef] [PubMed]
22. Tavakoly Sany, S.B.; Hashim, R.; Rezayi, M.; Salleh, A.; Safari, O. A review of strategies to monitor water and sediment quality for a sustainability assessment of marine environment. *Environ. Sci. Pollut. Res.* **2014**, *21*, 813–833. [CrossRef]
23. Xu, J.; He, S.; Wu, S.; Huang, J.; Zhou, W.; Chen, X. Effects of HRT and water temperature on nitrogen removal in autotrophic gravel filter. *Chemosphere* **2016**, *147*, 203–209. [CrossRef] [PubMed]
24. Hua, Z.; Wang, Y. Advance on the release of pollutants in river and lake sediments under hydrodynamic conditions. *J. Hohai Univ. (Nat. Sci.)* **2018**, *46*, 95–105. [CrossRef]
25. Wang, P.; Li, Q.; Cai, Y. Effect of sediment resuspension on BPA adsorption in Taihu Lake. *Water Resour. Prot.* **2015**, *31*, 35–41. [CrossRef]
26. Bai, G.; Zhang, Y.; Yan, P.; Yan, W.; Kong, L.; Wang, L.; Wang, C.; Liu, Z.; Liu, B.; Ma, J.; et al. Spatial and seasonal variation of water parameters, sediment properties, and submerged macrophytes after ecological restoration in a long-term (6 year) study in Hangzhou west lake in China: Submerged macrophyte distribution influenced by environmental variables. *Water Res.* **2020**, *186*, 116379. [CrossRef]
27. Liu, Z.; Li, W.; Zhang, X.; Zhang, K.; Chen, S.; Xiong, W. Influence of Submerged Macrophytes on Phosphorus Transference between Overlying Water and Sediment in the Growth Period under Static and Flowing Conditions. *Res. Environ. Sci.* 2022, *in press*. [CrossRef]
28. Diaz, R.J.; Rutger, R. Spreading Dead Zones and Consequences for Marine Ecosystems. *Science* **2008**, *321*, 926–929. [CrossRef]
29. Robert, A.R.; Suvasis, D.; Kate, M.C.; Adam, D.J.; Janet, G.H.; Peggy, A.O. Arsenic sequestration by sorption processes in high-iron sediments. *Geochim. Cosmochim. Acta* **2007**, *71*, 5782–5803. [CrossRef]
30. Han, C.; Ding, S.; Yao, L.; Shen, Q.; Zhu, C.; Wang, Y.; Xu, D. Dynamics of phosphorus-iron-sulfur at the sediment-water interface influenced by algae blooms decomposition. *J. Hazard. Mater.* **2015**, *300*, 329–337. [CrossRef]
31. Shen, Q.; Cheng, L.; Zhou, Q.; Shang, J.; Zhang, L.; Fan, C. Effects of physical and chemical characteristics of surface sediments in the formation of shallow lake algae-induced black bloom. *J. Environ. Sci.* **2013**, *25*, 2353–2360. [CrossRef]
32. Galloway, J.N.; Townsend, A.R.; Erisman, J.W.; Bekunda, M.; Cai, Z.; Freney, J.R.; Martinelli, L.A.; Seitzinger, S.P.; Sutton, M.A. Transformation of the Nitrogen Cycle: Recent Trends, Questions, and Potential Solutions. *Science* **2008**, *320*, 889–892. [CrossRef] [PubMed]
33. Liu, W.R.; Zhao, J.L.; Liu, Y.S.; Chen, Z.F.; Yang, Y.Y.; Zhang, Q.Q.; Ying, G.G. Biocides in the Yangtze River of China: Spatiotemporal distribution, mass load and risk assessment. *Environ. Pollut.* **2015**, *200*, 53–63. [CrossRef] [PubMed]
34. Chavan, P.V.; Dennett, K.E.; Marchand, E.A. Behavior of Pilot-Scale Constructed Wetlands in Removing Nutrients and Sediments Under Varying Environmental Conditions. *Water Air Soil Pollut.* **2008**, *192*, 239–250. [CrossRef]
35. Wei, D.; Singh, R.P.; Li, Y.; Fu, D. Nitrogen removal efficiency of surface flow constructed wetland for treating slightly polluted river water. *Environ. Sci. Pollut. Res.* **2020**, *27*, 24902–24913. [CrossRef]
36. Hollander, M.; Wolfe, D.A.; Chicken, E. *Nonparametric Statistical Methods*, 3rd ed.; John Wiley & Sons, Inc.: Hoboken, NJ, USA, 2015; pp. 451–494.
37. Ma, S.; Wang, H.; Wang, H.; Zhang, M.; Li, Y.; Bian, S.; Liang, X.; Søndergaard, M.; Jeppesen, E. Effects of nitrate on phosphorus release from lake sediments. *Water Res.* **2021**, *194*, 116894. [CrossRef]
38. Kheirollahpour, M.; Shohaimi, S.; Marchini, J.S. Dimensional Model for Estimating Factors influencing Childhood Obesity: Path Analysis Based Modeling. *Sci. World J.* **2014**, *2014*, 512148. [CrossRef] [PubMed]
39. Kpolovie, P. *Statistical Analysis with SPSS for Research*, 1st ed.; ECRTD Publication: London, UK, 2017; pp. 355–392; ISBN 978-1-5272-0701-1.
40. Niu, T.; Zhou, Z.; Shen, X.; Qiao, W.; Jiang, L.; Pan, W.; Zhou, J. Effects of dissolved oxygen on performance and microbial community structure in a micro-aerobic hydrolysis sludge in situ reduction process. *Water Res.* **2016**, *90*, 369–377. [CrossRef]
41. Wu, Y.; Wen, Y.; Zhou, J.; Wu, Y. Phosphorus release from lake sediments: Effects of pH, temperature and dissolved oxygen. *KSCE J. Civ. Eng.* **2014**, *18*, 323–329. [CrossRef]
42. Fan, J.H.; Liu, X.Y.; Gu, Q.Y.; Zhang, M.J.; Hu, X.W. Effect of hydraulic retention time and pH on oxidation of ferrous iron in simulated ferruginous acid mine drainage treatment with inoculation of iron-oxidizing bacteria. *Water Sci. Eng.* **2019**, *12*, 213–220. [CrossRef]

43. Li, Y.; Xia, B.; Zhang, J.; Li, C.; Zhu, W. Assessing high resolution oxidation-reduction potential and soluble reactive phosphorus variation across vertical sediments and water layers in Xinghu Lake: A novel laboratory approach. *J. Environ. Sci.* **2010**, *22*, 982–990. [CrossRef]
44. Hamersley, M.R.; Howes, B.L. Control of denitrification in a septage-treating artificial wetland: The dual role of particulate organic carbon. *Water Res.* **2002**, *36*, 4415–4427. [CrossRef] [PubMed]
45. Søndergaard, M.; Jensen, J.P.; Jeppesen, E. Role of sediment and internal loading of phosphorus in shallow lakes. *Hydrobiologia* **2003**, *506*, 135–145. [CrossRef]
46. Fu, K.; Yang, F.; Jin, Y.; Liu, L.; Yang, Z.; Chou, F. Effect of intermittent aeration strategy based on dissolved oxygen and anoxic period regulation on partial nitrification process. *Chin. J. Environ. Eng.* **2022**, *16*, 824–836. [CrossRef]
47. Xu, W.; Gu, G.; Chen, Y. Research on Effect of SRT on A/A/O Biological Nutrient Removal and Simulation. *Technol. Water Treat.* **2007**, *33*, 68–71. [CrossRef]
48. Denis, L.; Grenz, C.; Alliot, É.; Rodier, M. Temporal variability in dissolved inorganic nitrogen fluxes at the sediment-water interface and related annual budget on a continental shelf (NW Mediterranean)Variabilité temporelle des flux d'azote inorganique dissous à l'interface eau–sédiment et bilan annuel sur un plateau continental (Méditerranée nord occidentale). *Oceanol. Acta* **2001**, *24*, 85–97. [CrossRef]
49. Trimmer, M.; Nedwell, D.B.; Sivyer, D.B.; Malcolm, S.J. Seasonal organic mineralisation and denitrification in intertidal sediments and their relationship to the abundance of *Enteromorpha* sp. and *Ulva* sp. *Mar. Ecol. Prog. Ser.* **2000**, *203*, 67–80. [CrossRef]
50. Chen, Z.; Chen, N.; Wu, Y.; Mo, Q.; Zhou, X.; Lu, T.; Tian, Y. Sediment-water Flux and Processes of Nutrients and Gaseous Nitrogen Release in a China Reservoir. *Environ. Sci.* **2014**, *35*, 3325–3335. [CrossRef]
51. Jing, L.D.; Wu, C.X.; Liu, J.T.; Wang, H.G.; Ao, H.Y. The effects of dredging on nitrogen balance in sediment-water microcosms and implications to dredging projects. *Ecol. Eng.* **2013**, *52*, 167–174. [CrossRef]
52. Yuan, H.; Huang, S.; Yuan, J.; You, Y.; Zhang, Y. Characteristics of microbial denitrification under different aeration intensities: Performance, mechanism, and co-occurrence network. *Sci. Total Environ.* **2021**, *754*, 141965. [CrossRef]
53. Bohlen, L.; Dale, A.W.; Sommer, S.; Mosch, T.; Hensen, C.; Noffke, A.; Scholz, F.; Wallmann, K. Benthic nitrogen cycling traversing the Peruvian oxygen minimum zone. *Geochim. Cosmochim. Acta* **2011**, *75*, 6094–6111. [CrossRef]
54. Beman, J.M.; Vargas, S.M.; Wilson, J.M.; Perez-Coronel, E.; Karolewski, J.S.; Vazquez, S.; Yu, A.; Cairo, A.E.; White, M.E.; Koester, I.; et al. Substantial oxygen consumption by aerobic nitrite oxidation in oceanic oxygen minimum zones. *Nat. Commun.* **2021**, *12*, 7043. [CrossRef] [PubMed]